iScience, Volume *24*

Supplemental information

Energetic and structural features of SARS-CoV-2 N-protein co-assemblies with nucleic acids

Huaying Zhao, Di Wu, Ai Nguyen, Yan Li, Regina C. Adão, Eugene Valkov, George H. Patterson, Grzegorz Piszczek, and Peter Schuck

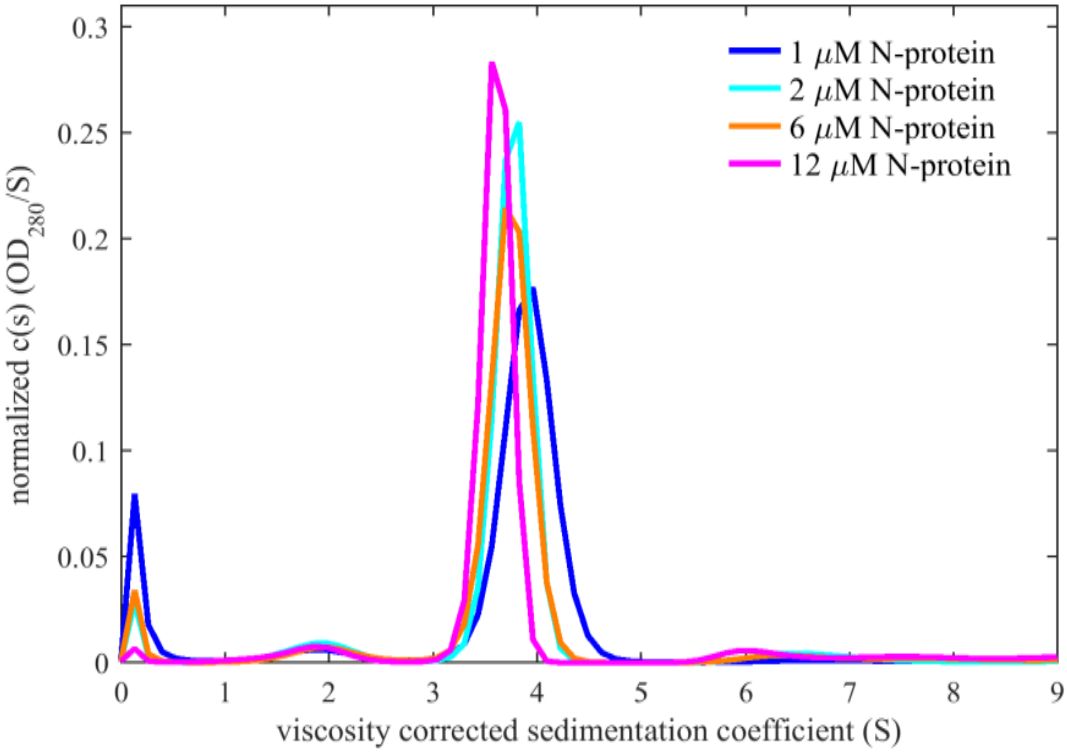

Figure S1: Lack of N-Protein dissociation at 10 °C, related to Figure 1

Sedimentation coefficient distributions of N-protein at 10 °C at different concentrations. Shown are normalized c(s) curves approximately corrected for viscosity ratio of water at 10 °C *vs* 20 °C (with remaining errors from temperature calibration uncertainties). Importantly, no concentration-dependent dissociation can be discerned (in contrast to conditions of **Figure S2**), with the small peak at 2 S representing a constant fraction of degraded protein. The slightly decreasing *s*-value at higher concentrations may be due to stronger hydrodynamic nonideality at lower temperatures, which is out of the scope of the present work.

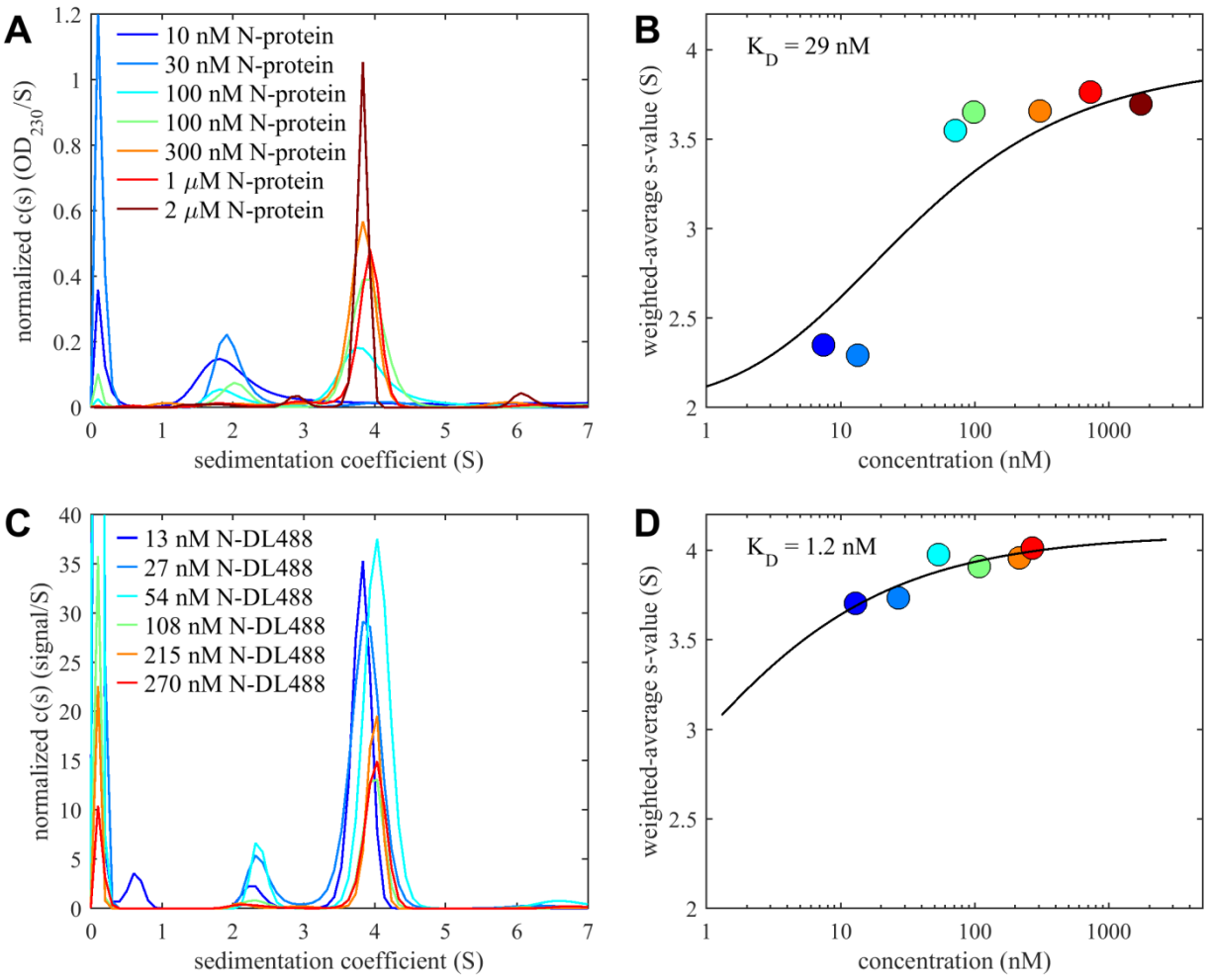

Figure S2: N-Protein Dimer Dissociation, related to Figure 1

(A) Sedimentation coefficient distributions of N-protein in PBS supplemented with 0.005% surfactant P20, obtained from SV-AUC experiments using far-UV detection at 230 nm. Shown are traces labeled with nominal loading concentrations (including a replicate at 100 nM).

(B) Isotherm of weight-average s-values of N-protein with P20 shown in Panel A, and best-fit monomer-dimer model. Concentrations are determined from integrated sedimentation boundary amplitudes.

(C) Sedimentation coefficient distributions of DyLight488-labeled N-protein in PBS based on SV-AUC using fluorescence detection (MacGregor et al., 2004; Zhao et al., 2013).

(D) Isotherm of weight-average s-values of DyLight-488-labeled N-protein in Panel C, and best-fit monomer-dimer model.

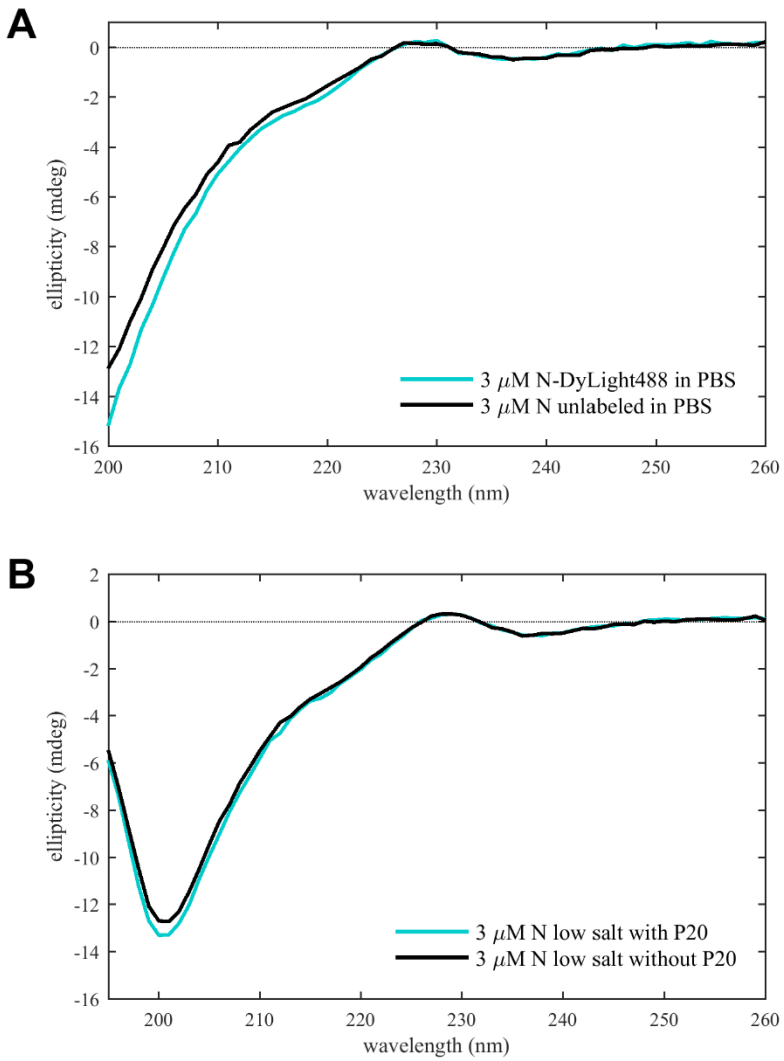

Figure S3: Circular Dichroism Spectra of N-protein with surfactant P20 or with fluorescent tag, related to Figure 1

(A) Comparison of CD spectra in PBS of unlabeled and DyLight488-labeled protein.

(B) Comparison of CD spectra of unlabeled N-protein in 12 mM KH_2PO_4/Na_2HPO_4, 3 mM KCl, 10 mM NaCl, pH 7.4 and in the same buffer supplemented with 0.005% P20.

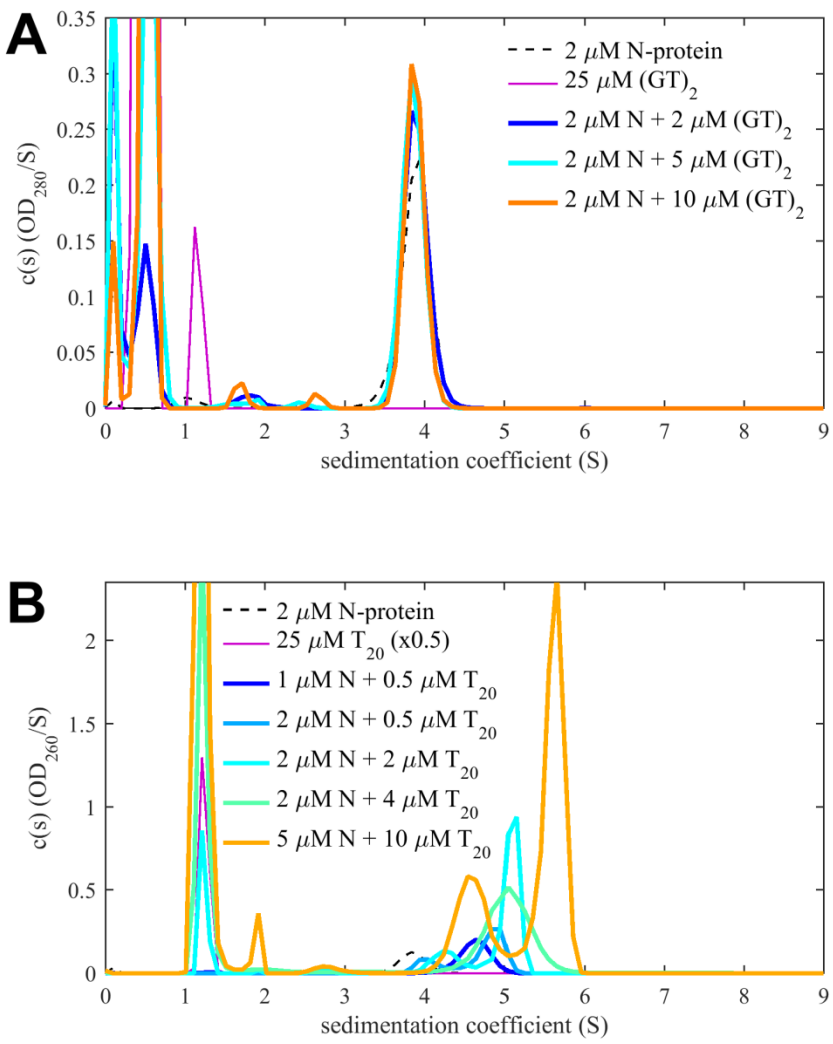

Figure S4: Oligonucleotide binding to N-protein in high salt buffer, related to Figure 2

(A) Sedimentation coefficient distributions of mixtures of N-protein and $(GT)_2$ in PBS show no increase in s-value and no significant increase in boundary amplitudes with $(GT)_2$ concentration.

(B) Concentration series of N-protein with T_{20} in PBS shows significant binding, but at strongly reduced level than in low salt buffer, exhibiting lower complex sedimentation coefficients. For presentation purpose, the values for the trace of 25 μM T_{20} (orange) are reduced by a factor of two.

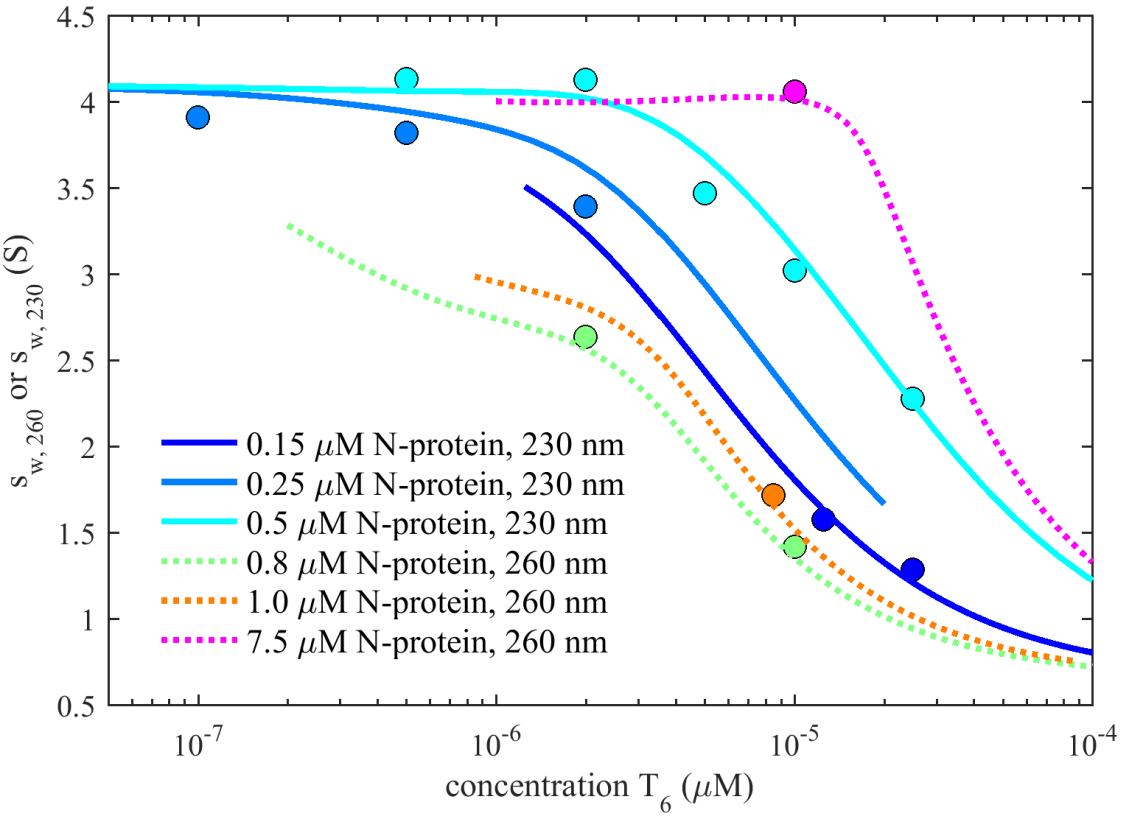

Figure S5: Binding isotherm analysis of N-protein binding T_6 in P20, related to Figure 3

Weight-average sedimentation coefficients of mixtures of N-protein and T_6 in PBS supplemented with 0.005% surfactant P20, obtained using far-UV detection at 230 nm (dark blue, light blue, and cyan) or 260 nm (green, red, magenta), respectively. The lines are from a global analysis simultaneously fitting all data points with a two-site binding model with *s*-values of complexes fixed to values calculated with hydrodynamic scaling laws accounting for the added mass of nucleic acid ligands to the N-protein dimer. Adjustable parameters were solely the affinities of the first and the second site, which converged to best-fit K_D-values of 0.29 and 4.1 μM, respectively.

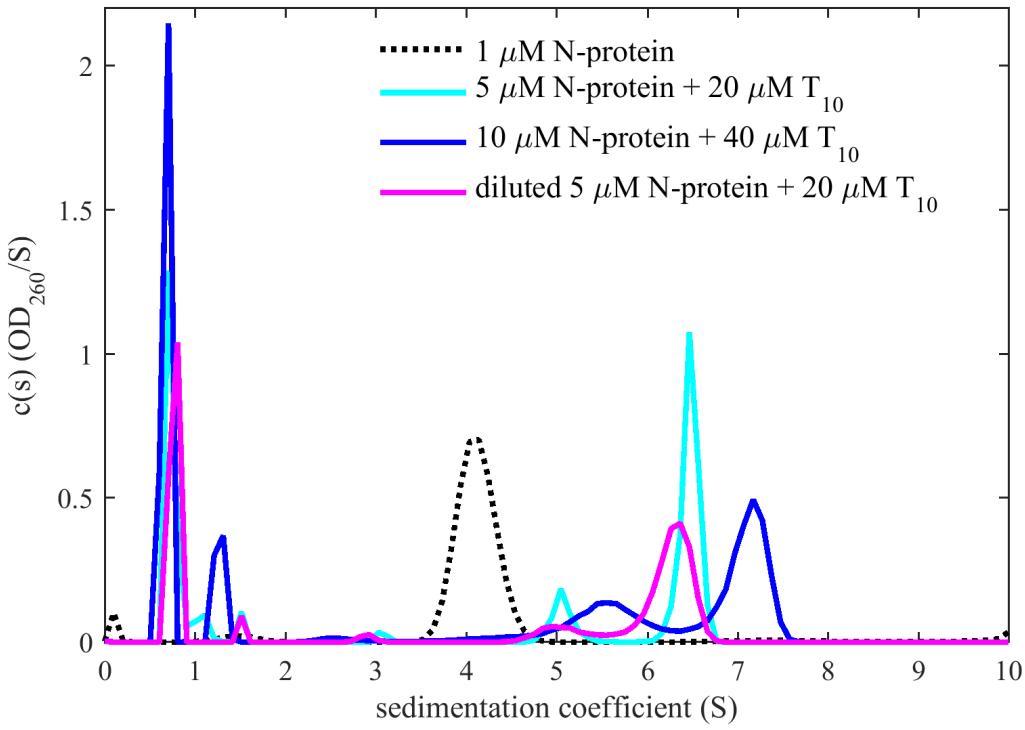

Figure S6: Reversibility of cloudiness and oligomerization with T_{10}, related to Figure 5

Sedimentation coefficient distributions of N-protein in different mixtures with T_{10} are shown. For reference, the dotted black line shows *c*(*s*) of 1 μM N-protein alone (observed at 280 nm, tenfold enhanced). The cyan line shows the bimodal reaction boundary distribution of 5 μM N-protein mixed with 20 μM T_{10}, with a peak at ≈6.4 S. Under this condition no cloudiness was observed, and the sedimenting signal of N-protein-containing (> 3 S) complexes was 0.290 OD_{260}. By contrast, significant cloudiness was observed immediately upon mixing 10 μM N-protein with 40 μM T_{10}. The corresponding *c*(*s*) distribution of this sample is shown in blue, exhibiting higher time-average sedimentation coefficients with a peak at ≈7.1 S. The total signal of N-protein containing species (> 3 S) is 0.390 OD_{260} – suggesting a significant loss of signal to the rapidly sedimenting dense phase. (We would expect twice the signal of the twofold lower concentrated sample, i.e., 0.580 OD_{260}). Prior to sedimentation, after ≈15 min of mixing, this sample was divided and an aliquot was diluted two-fold, to generate a new sample at nominally 5 μM N-protein with 20 μM T_{10}. Similar to the directly mixed sample at the same nominal concentration, this diluted sample was only slightly cloudy. In the SV experiment (alongside the directly mixed samples) the *c*(*s*) distribution exhibits a peak at ≈6.2 S (magenta), indicating oligomer dissociation upon dilution. The total visible sedimenting signal of the diluted sample (> 3 S) is 0.241 OD_{260}, which is significantly more than half the signal of the initially twofold more concentrated sample (expecting 0.195 OD_{260}), though less than the directly mixed sample. Reversibility of assembly in the diluted sample is indicated by 1) disappearance of cloudiness; 2) recovered signal of observable oligomeric protein/NA complex; 3) the decreased *s*-value of the diluted sample mimicking that of the directly mixed sample at the same concentration.

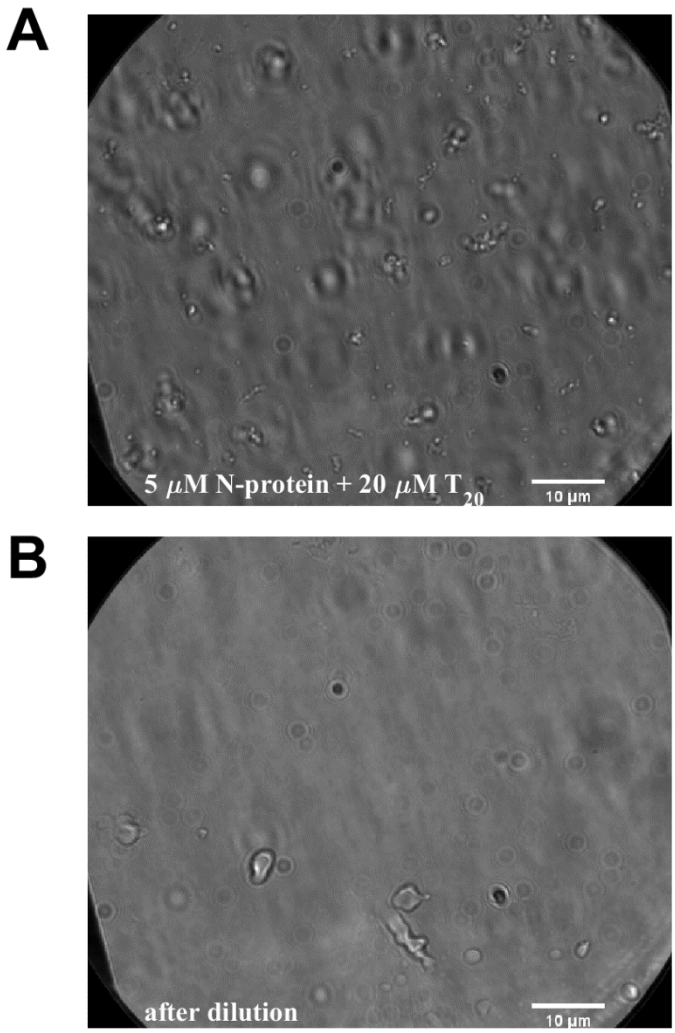

Figure S7: Reversibility of droplet formation of N-protein with T_{20}, related to Figure 5

Widefield microscopy image of 5 μM N-protein with 20 μM T_{20} before (A) and after (B) twofold dilution.

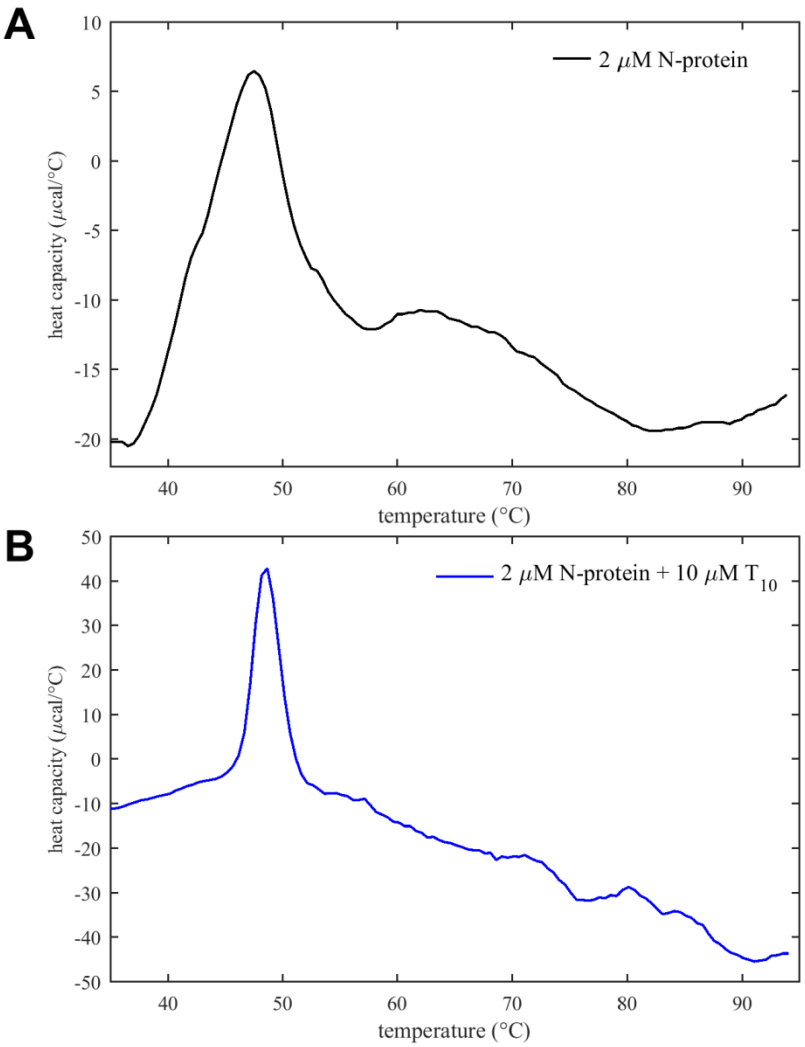

Figure S8: Differential scanning calorimetry of N-protein with T_{10}, related to Figure 7

Shown are DSC traces of 2 μM N-protein in the absence (A) and presence (B) of 10 μM T_{10} .

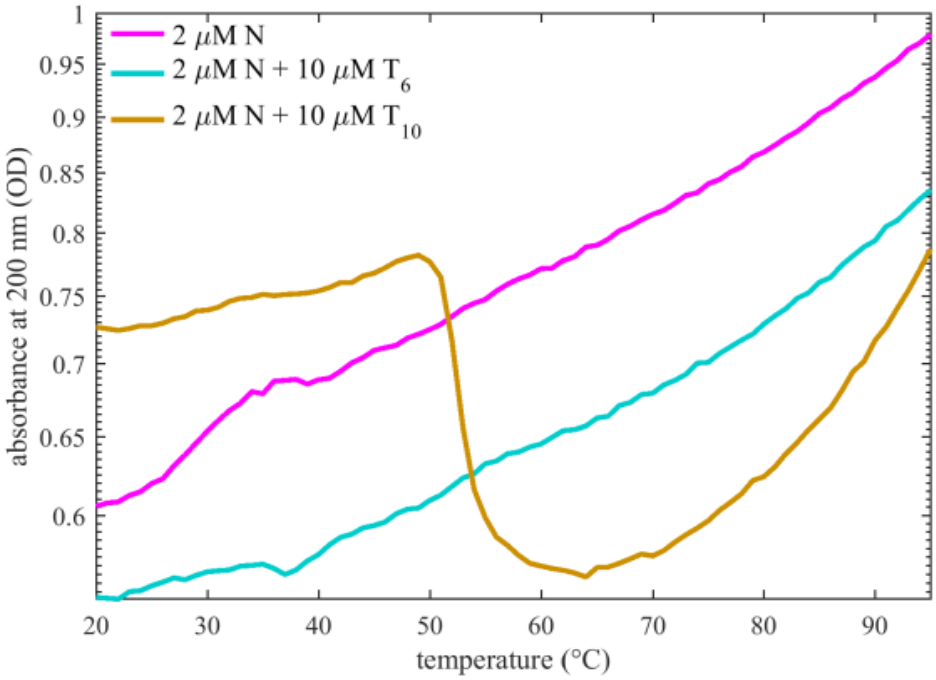

Figure S9: Far-UV absorbance during temperature scan, related to Figure 7

Absorbance traces at 200 nm recorded during CD temperature scans in **Figure 7**.

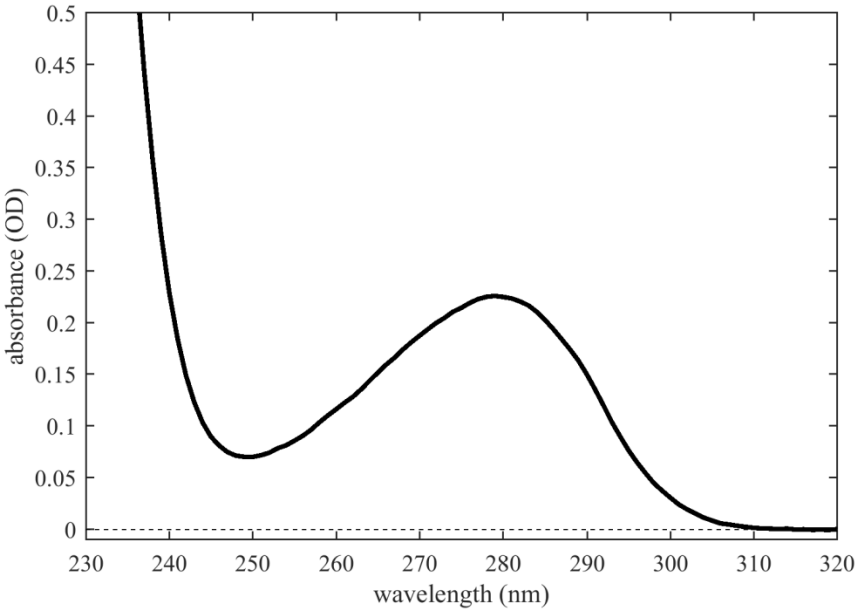

Figure S10: Absorbance spectrum of N-protein, related to STAR Methods

Shown is a 1:10 dilution of N-protein stock solution after dialysis against working buffer.